CALCULATION OF CONCENTRATION-DEPENDENT MUTUAL DIFFUSION COEFFICIENT IN DESORPTION OF FILM

YUJI SANO AND SHUICHI YAMAMOTO
Department of Chemical Engineering,
Yamaguchi University, Ube 755

Key Words: Mass Transfer, Desorption, Drying, Mutual Diffusion Coefficient, Polymer Solution, Food Aqueous Solution

For the isothermal desorption of film, the diffusion equation for a slab based on the dissolved solid coordinate is solved numerically with various types of concentration dependence of the diffusion coefficient. Based on the assumption of concentration distribution similarity, the relations between desorption rate and integral average diffusion coefficient are derived as functions of the ratios of average concentration to center concentration for both the penetration period and the regular regime, regardless of the type of concentration dependence of the diffusion coefficient. By means of these relations, Methods of calculating the diffusion coefficient as a function of solvent concentration are presented for both the initial rate in the penetration period and the rate in the regular regime, which covers the whole concentration range included in the desorption data. The method is usable within an error of 10% in the range of 0.5< (the ratio of average concentration to center concentration)<0.9, which covers a variety of concentration dependences of the diffusion coefficient.

Introduction

When analysing the drying process of solutions such as polymer solutions and aqueous solutions of food, it is important to know their mutual diffusion coefficients, which usually show strong concentration dependence. Sorption experiments are commonly used to obtain the diffusion coefficient. In some polymer-solvent systems near their glass transition point, non-Fickian behaviour such as a sigmoidal sorption curve due to time-dependent relaxation of polymer chains are found in the adsorption, while the desorption is quite Fickian.[10] In such systems, only desorption experiments can be used to obtain the diffusion coefficient.

Methods of calculating the concentration-dependent mutual diffusion coefficient for sorption experiments were reviewed by Crank[2] and Vrentas and Duda.[9] Recently, Schoeber and Thijssen[8] proposed a shortcut method for the calculation of drying rates for slabs with concentration-dependent diffusion coefficient. They introduced the concept of regular regime in the drying analysis and proposed a method for calculating the diffusion coefficient from the regular-regime drying curve. Vrentas and Duda[9] proposed a method for calculating the diffusion coefficient from the initial rate in step-change sorption experiments, assuming exponential concentration dependence of the diffusion coefficient. The authors[12] proposed a method by correlating the apparent diffusion coefficient to the weighted mean diffusion coefficient proposed by Crank[1].

Most previous calculation methods seem to utilize only a part of the information included in the sorption data[9] and have some shortcomings such as cumbersome calculation and application in a limited concentration range.

In this paper, a method for calculating the diffusion

Received August 21, 1989. Correspondence concerning this article should be addressed to Y. Sano.

coefficient covering the whole concentration range concerned in desorption experiments, regardless of the type of concentration dependence, and based on the assumption of similar concentration distribution on a slab is described.

1. Governing Equations for Desorption

1.1 Diffusion equations

The diffusion equation for a slab based on the dissolved-solid coordinates[4,5] is

$$\frac{\partial m}{\partial \tau}=\frac{\partial}{\partial \phi}\left[D_r\frac{\partial m}{\partial \phi}\right] \tag{1}$$

By using Eq. (1), the effects of volume change due to diffusion and the moving-boundary problem due to solvent loss are treated automatically.[7]

The desorption process considered here is the case in which the initial concentration is uniform, the rate of desorption is controlled entirely by the internal diffusion of solvent, and the surface concentration is zero. Then the initial condition and the boundary conditions are

$$\tau=0\,,\qquad m=1 \tag{2}$$

$$\phi=0\,,\qquad \frac{\partial m}{\partial \phi}=0 \tag{3}$$

$$\phi=1\,,\qquad m=0 \tag{4}$$

where

$$\phi=\frac{z}{Z} \tag{5}$$

$$z=\int_0^r \rho_s dr \tag{6}$$

$$Z=\int_0^R \rho_s \mathrm{d}r=\rho_{s0}R_0=R_s d_s \tag{7}$$

$$\tau=\frac{D_0\rho_{s0}^2}{d_s^2R_s^2}t \tag{8}$$

$$D_r=\frac{D\rho_s^2}{D_0\rho_{s0}^2} \tag{9}$$

$$m=\frac{u}{u_0} \tag{10}$$

$$\rho_s=\frac{d_s d_m}{ud_s+d_m} \tag{11}$$

The desorption rate is

$$F=-\left(D_r\frac{\partial m}{\partial \phi}\right)_{\phi=1}=\frac{dE}{d\tau} \tag{12}$$

$$E=1-\bar{m}=1-\int_0^1 m d\phi \tag{13}$$

Table 1. Concentration Dependence of D_r

(1) $D_r=m^a \quad 0\leqq a\leqq 5$
(2) $D_r=\exp(a(m-1)) \quad -3\leqq a\leqq 5$
(3) $D_r=am+(1-a) \quad -10\leqq a<1$
(4) skim milk-water system at 303 K[11]
$d_s=1580$ [kg/m^3] $d_m=1000$ [kg/m^3]
$D=\exp\left(-\dfrac{38.92+323.39\omega_m}{1+15.84\omega_m}\right)$ [m^2/s], $\omega_m\leqq 0.9$
(5) Polyvinyl alcohol (PVA)-water system at 323 K[6]
$d_f=1270$ [kg/m^3] $d_m=1000$ [kg/m^3]
$D=\exp\left(-\dfrac{33.0+360\omega_m}{1+16.0\omega_m}\right)$ [m^2/s], $\omega_m\leqq 0.8$

Eq. (1) with Eqs. (2), (3) and (4) is solved numerically by the Crank-Nicolson finite difference method, using various types of concentration-dependence equations for the diffusion coefficient.

1.2 The concentration-dependent diffusion coefficient

The mutual diffusion coefficients for polymer solutions and aqueous solutions of food material usually decrease continuously with solvent concentration. However, in some polymer-solvent systems such as the toluene-polystyrene system[3] the diffusion coefficient changes with concentration and shows a maximum value.

The reduced diffusion coefficient D_r considered here includes solid concentration ρ_s as shown in Eq. (9). D_r varies with concentration not only by the concentration dependence of D itself but also by the term ρ_s. The concentration dependences of D_r tested in this work, are the three mathematical model equations and two empirical equations listed in **Table 1** and shown in **Fig. 1**.

In the skim milk-water system ($d_s>d_m$), the diffusion coefficient decreases continuously with decreasing water concentration in the whole concentration range, but D_r in this system shows a maximum for initial water mass fraction $\omega_{m0}>0.5$.

2. Flux Equations Based on Concentration Distribution Similarity

The desorption process presented by Eqs. (1), (2), (3) and (4) is divided into three periods, as shown in **Fig. 2**. In the following, the penetration period, the transition period and the regular regime are abbreviated as PP, TP and RR respectively.

In PP, the desorption process can be considered as a diffusion process in a semi-infinite medium, and the following equation is obtained by introducing Boltzmann's transformation into Eq. (1).

$$2\xi\frac{dm}{d\xi}+\frac{d}{d\xi}\left(D_r\frac{dm}{d\xi}\right)=0 \tag{14}$$

$$\xi=\frac{1-\phi}{2\sqrt{\tau}} \tag{15}$$

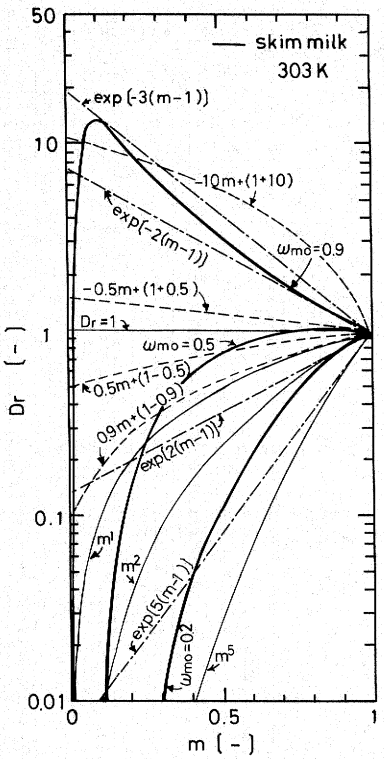

Fig. 1. Concentration dependence of D_r

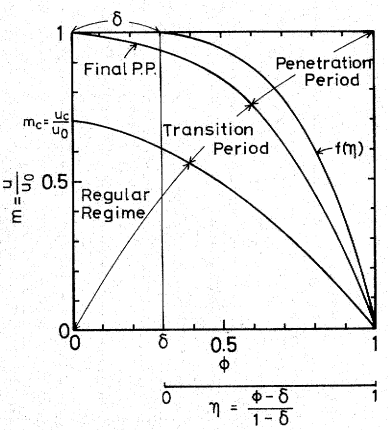

Fig. 2. Concentration distributions of penetration period, transition period and regular regime

The reduced solvent content m is a function of ξ alone and thus the distribution of m is strictly similar in the range of $\delta<\phi<1$. In PP, the plot of E vs. $\sqrt{\tau}$ is linear with a constant slope of β regardless of the concentration dependence of D_r.[7)]

$$F=-\left(D_r\frac{\partial m}{\partial\phi}\right)_{\phi=1}=\frac{1}{2\sqrt{\tau}}\int_0^1 2\xi dm=\frac{\beta}{2\sqrt{\tau}} \tag{16}$$

$$\beta=\frac{dE}{d\sqrt{\tau}} \tag{17}$$

$$FE=\frac{1}{2}\beta^2 \tag{18}$$

Here, we consider the concentration distribution function based on the similarity.

$$\frac{m}{m_c}=\frac{u}{u_C}=f(\eta) \tag{19}$$

$$\eta=\frac{\phi-\delta}{1-\delta} \tag{20}$$

where $1-\delta$ is the penetration depth as shown in Fig. 2. Next, we consider a variable Y, which is a dimensionless flux in the slab.

$$Y(\phi)=-D_r\frac{\partial m}{\partial\phi} \tag{21}$$

At the surface

$$Y=-\left(D_r\frac{\partial m}{\partial\phi}\right)_{\phi=1}=F \tag{22}$$

The average flux in the slab is obtained by the integration of Eq. (21).

$$\bar{Y}=\int_0^1 Y d\eta=\frac{1}{1-\delta}\int_0^{m_c} D_r dm=\frac{m_c\overline{D_{rs}}}{1-\delta} \tag{23}$$

where the integral average diffusion coefficient is

$$\overline{D_{rc}}=\frac{1}{m_c}\int_0^{m_c} D_r dm=\frac{1}{u_c}\int_0^{u_c}\frac{D\rho_c^2}{D_0\rho_{s0}^2}du \tag{24}$$

On the other hand, by putting Eq. (21) into Eq. (1) and after some manipulation the flux ratio $\bar{Y}/F$ is expressed by the average value and the first moment of the reduced concentration distribution. (See **Appendix**)

Finally, we obtain the following equations for the end point of PP

$$\frac{\overline{D_{rc}}}{F}=\frac{1-2\bar{f}_{pp}+2M_{pp}}{(1-\bar{f}_{pp})} \tag{25}$$

$$M_{pp}=\int_0^1 \eta f(\eta)d\eta \tag{26}$$

$$\bar{f}_{pp}=\int_0^1 f(\eta)d\eta \tag{27}$$

$\bar{f}_{pp}$ is constant during PP because of the similarity of concentration distribution in the range $0\leqq\eta\leqq1$ ($\delta\leqq\phi\leqq1$) and can be obtained by the following equation from the value of E at the end point of PP because $\delta=0$ at this point.

$$1-\bar{f}_{pp}=\frac{E}{1-\delta}=\frac{1-\bar{m}}{1-\delta} \tag{28}$$

After PP, the concentration distribution changes gradually from the pattern of PP to the pattern of RR. If we assume the similarity of concentration distirbution in RR using Eqs. (19) and (20) in which $\delta=0$ and $\eta=\phi$ (the function of Eq. (19) may be

different in PP and RR), we get the following equations for RR. (see **Appendix**)

$$\frac{m_c\overline{D_{rc}}}{F}=1-\frac{M_{RR}}{\bar{f}_{RR}} \tag{29}$$

$$M_{RR}=\int_0^1 \phi f(\phi)d\phi \tag{30}$$

$$\bar{f}_{RR}=\frac{\bar{m}}{m_c}=\int_0^1 f(\phi)d\phi \tag{31}$$

3. Results and Discussion

The results of numerical solutions of Eq. (1) with Eqs. (2), (3) and (4), using the various types of D_r shown in Table 1, are analysed under the consideration of the flux equations described above.

3.1 PP, TP and RR during desorption

Examples of the numerical solutions are shown by the plots of $E, \bar{f}$ and m_c, vs. $\sqrt{\tau}$ in **Figs. 3 and 4**. E vs. $\sqrt{\tau}$ shows a linear relation with a slope of β in PP. The linear relation continues for a while after m_c begins to fall from unity. At a certain later τ, the relation E vs. $\sqrt{\tau}$ begins to deviate from the straight line as shown by the solid circle keys. These points can be considered as the starting point of RR and are conveniently determined here by the point at which $F\cdot E$ is 90% of $(F\cdot E)_{PP}$.

The end-points of PP, defined as the point at which m_c begins to fall from unity, is here taken practically as the point $m_c=0.99$ and are shown by the open circle keys. The period between the end point of PP and the starting point of RR is TP.

3.2 Concentration distribution and the ratio of the average to the center concentration $\bar{f}$

Several samples of comparisons between concentration distributions at the end of point of PP and the starting point of RR are shown in **Fig. 5**.

$\bar{f}$ is considered as the representative value of the concentration distribution.

In PP, $\bar{f}$ is given by the following equation.

$$\bar{f}=\delta+(1-\delta)\bar{f}_{PP}=\bar{m} \tag{32}$$

$\bar{f}_{PP}$, given by Eq. (27), corresponds to the value of $\bar{f}$ at the end of PP. The change of $\bar{f}$ with $\sqrt{\tau}$ is linear in PP, which corresponds to the linear change of δ with $\sqrt{\tau}$. In TP, the change of $\bar{f}$ is small for continuously decreasing D_r with m. But when D_r has a maximum value or increases with decreasing m, large changes in $\bar{f}$ are found, as shown in Fig. 4.

In RR, the change in $\bar{f}$ given by Eq. (31) is generally very small. For the case of $D_r=m^a$, $\bar{f}$ is essentially constant in RR. This means that strict similarity of concentration distribution holds in this case. The constancy of $\bar{f}$ in RR reflects the adequacy of the assumption of similarity in RR.

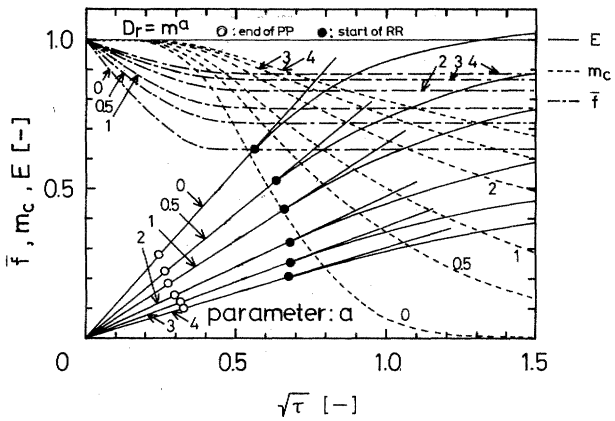

Fig. 3. $E, \bar{f}$ and m_c vs. $\sqrt{\tau}$ for $D_r=m^a$

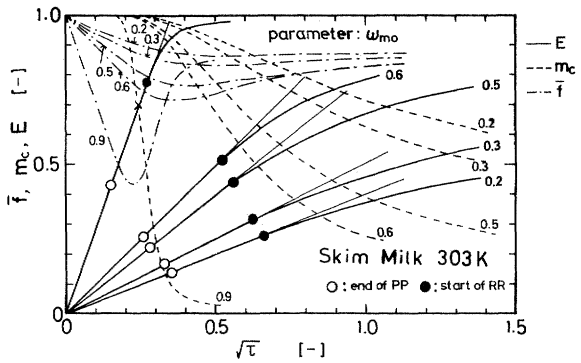

Fig. 4. $E, \bar{f}$ and m_c vs. $\sqrt{\tau}$ for skim milk-water system

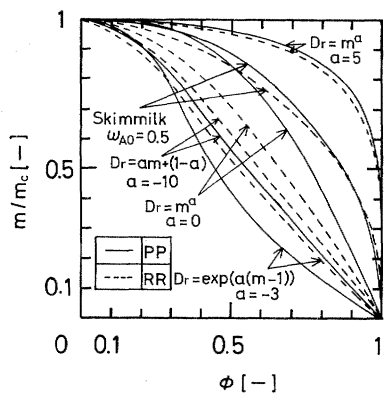

Fig. 5. Comparison of reduced concentration distribution in PP and RR

The change in $\bar{f}$ is correlated by the term $d\ln F/d\ln\bar{m}$. In PP, we obtain the following equation by the differentiation of Eq. (18).

$$\frac{d\ln F}{d\ln\bar{m}}=\frac{1-E}{E}=\frac{\bar{f}}{1-\bar{f}} \tag{33}$$

In RR, the following equation is empirically obtained regardless of the concentration dependence of D_r, as shown in **Fig. 6**

$$\frac{1}{\bar{f}_{RR}}=1+0.643\left(\frac{d\ln\bar{m}}{d\ln F}\right)-0.10\left(\frac{d\ln\bar{m}}{d\ln F}\right)^2 \tag{34}$$

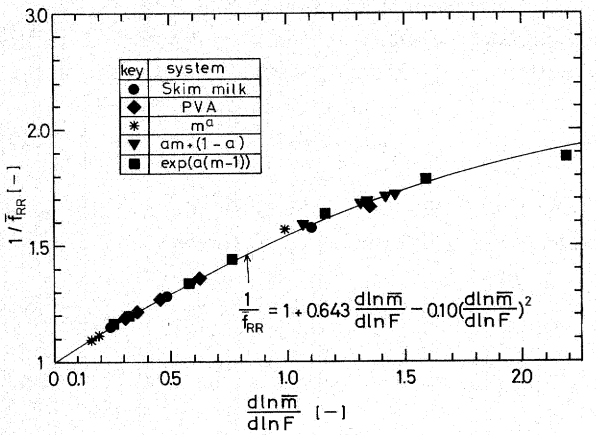

Fig. 6. $1/\bar{f}_{RR}$ vs. $d\ln\bar{m}/d\ln F$

The convergence of $\bar{f}$ to Eq. (34) in RR is quite satisfactory. The small changes in $\bar{f}$ in RR correspond well to Eq. (34) with errors less than 3% for $\bar{f}_{RR}>0.5$. Then the center value m_c is calculated from the observed value of $\bar{m}$ with $\bar{f}_{RR}$ by Eq. (34) through RR.

3.3 Relation between M and $\bar{f}$

The first moment M and the average value $\bar{f}$ of the concentration distribution given by Eqs. (26) and (27) for PP and Eqs. (30) and (31) for RR, respectively are calculated from the numerical solutions of concentration distribution. All values of M and $\bar{f}$ of the concentration distribution in PP and RR are correlated surprisingly well by the following equation, regardless of the type of D_r, as shown in **Fig. 7**.

$$M=0.235\bar{f}^2+0.362\bar{f}-0.0965 \quad (0.5<\bar{f}<1) \quad (35)$$

By using Eq. (35) we can obtain the relation between the integral average diffusion coefficient and the desorption rate. For PP, we adopt the practical end point of $m_c=0.99$ and then from Eqs. (18) and (25), we obtain (see **Appendix**)

$$\frac{m_c\overline{D_{rc}}}{1/2\beta^2}=\frac{0.807-0.470\bar{f}_{PP}}{1-0.99\bar{f}_{PP}} \quad (36)$$

For RR, from Eq. (29)

$$\frac{m_c\overline{D_{rc}}}{F}=0.0965/\bar{f}_{RR}+0.639-0.235\bar{f}_{RR} \quad (37)$$

The numerical results of $m_c\overline{D_{rc}}/(1/2\beta^2)$ vs. $\bar{f}_{PP}$ for PP and $m_c\overline{D_{rc}}/F$ vs. $\bar{f}_{RR}$ for RR are plotted in **Figs. 8 and 9** respectively. The errors in Eq. (36) for PP may be attributed partly to the definition of the end-point of PP. The errors in Eq. (37), which may be attributed to the assumption of similarity of the concentration distribution in RR, are up to 10% at the beginning of RR and become smaller in the later RR. If the following empirical equation is used instead of Eq. (37), the errors become smaller, as shown in Fig. 9.

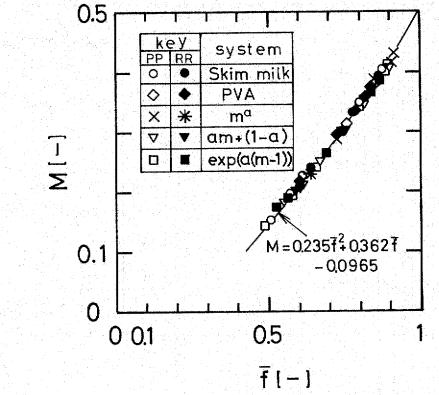

Fig. 7. M *vs.* $\bar{f}$ for PP and RR

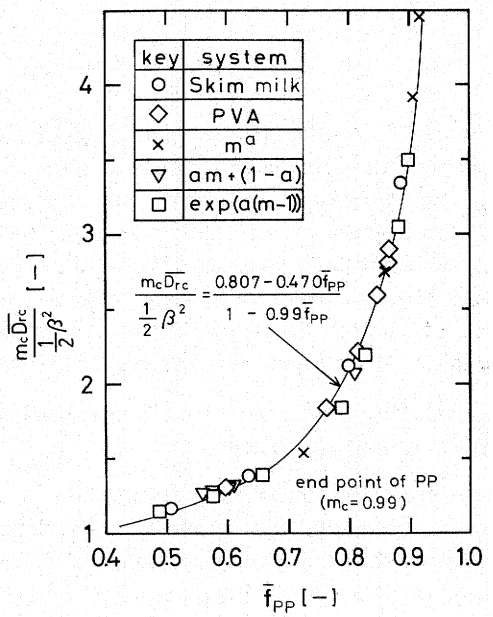

Fig. 8. $m_c\overline{D_{rc}}/(\beta^2/2)$ vs. $\bar{f}_{PP}$

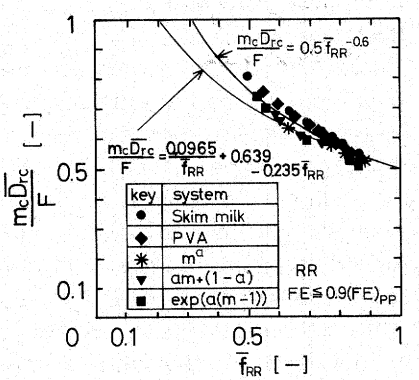

Fig. 9. $m_c\overline{D_{rc}}/F$ vs. $\bar{f}_{RR}$

$$\frac{m_c\overline{D_{rc}}}{F}=0.50\bar{f}_{RR}^{-0.60} \quad (38)$$

3.4 The empirical relation of β vs. $\bar{f}_{PP}$

From the numerical solutions, the initial slope of E vs. $\sqrt{\tau}$ in PP is plotted with $1/\bar{f}_{PP}$ as shown in **Fig. 10** and is presented by the following equation.

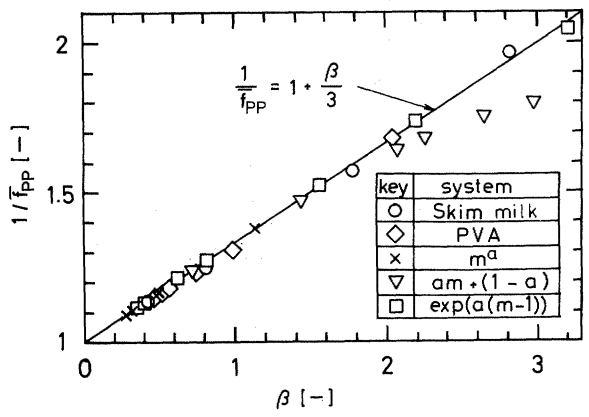

Fig. 10. $1/\bar{f}_{PP}$ vs. β

$$\frac{1}{\bar{f}_{PP}} = 1 + \beta/3 \tag{39}$$

The errors in Eq. (39) are less than 3% for $\bar{f}_{PP} > 0.5$ regardless of the functional form of D_r except the in case of $Dr = am + (1-a)$, in which the error becomes up to 10% for $a = -10$ as shown in Fig. 10. In the systems of skim milk-water and PVA-water, Eq. (39) can be used quite satisfactorily in the range considered.

Note that β is the slope of E vs. $\sqrt{\tau}$ in PP for the normalized D_r, in which $D_r = 1$ at $m = 1$.

4. Calculation Procedure for Concentration Dependent Diffusion Coefficient

The correlation equations presented above can be used for calculation of the concentration dependent diffusion coefficients from the data of desorption experiments at a constant temperature. The calculation is conveniently performed by using the following values: $D'_r = D\rho_s^2$ instead of D_r, $F' = dE/d\tau'$ instead of F, and $\tau' = t/d_s^2 R_s^2$ instead of τ.

4.1 Calculation procedure

The desorption data are treated as follows.

1) From desorption experiments with various values of initial solvent concentration u_0, the change of $\bar{u}$ with time are obtained.

2) $E = 1 - \bar{m}$ vs. $\sqrt{\tau'}$ is plotted. The initial part of this plot shows a linear relation through the origin. The slope of the relation gives $\beta' = dE/d\sqrt{\tau'}$ in PP.

3) The starting point of RR is conveniently estimated by the point at which the plot of E vs. $\sqrt{\tau'}$ begins to deviate from the linear relation. During RR, F' is calculated for various values of $\bar{u}$ by the differentiation of E vs. $\sqrt{\tau'}$.

4) $F'u_0$ obtained from the experiments of the various u_0 values are plotted together with $\bar{u}$ in log-log form. The plots make one master curve of the desorption rate in RR which is independent of the initial concentrations as shown by Schoeber.[7]

From these data, the following three ways of calculating the diffusion coefficient can be utilized.

(1) Direct calculation of $D\rho_s^2$ in PP

The value of $D_0\rho_{s0}^2$ is usually unknown. If we use $\beta' = dE/d\sqrt{\tau'}$ instead of $\beta = dE/d\sqrt{\tau}$, then

$$\left(\frac{\beta'}{\beta}\right)^2 = D_0\rho_{s0}^2 \tag{40}$$

From Eqs. (18), (36), (39) and (40), the following equations are obtained. (see **Appendix**)

$$D_0\rho_{s0}^2 = \frac{X\gamma}{2}\beta'^2 \tag{41}$$

where $D_o\rho_{s0}^2$ is the value of $D\rho_s^2$ at u_0 (strictly at $0.99u_0$) and

$$X = \frac{0.870 - 0.470\bar{f}_{PP}}{1 - 0.99\bar{f}_{PP}} \tag{42}$$

$$\gamma = 1 + 2\frac{d\ln\beta'}{d\ln u_0} + \frac{d\ln X}{d\ln u_0} = \frac{0.233\bar{f}_{PP}^2}{(1-\bar{f}_{PP})(0.807 - 0.470\bar{f}_{PP})} \tag{43}$$

In this derivation the approximation

$$(1 - 0.99\bar{f}_{PP})/(1 - \bar{f}_{PP}) = 1.05 \qquad \text{for } \bar{f}_{PP} < 0.9$$

is used.

$\bar{f}_{PP}$ and $D_0\rho_{s0}^2$ are obtained by trial calculation. First, the values of β' are plotted with u_0 in log-log form and $d\ln\beta'/d\ln u_0$ is obtained. Next, calculate $\bar{f}_{PP}$ as the first approximation by Eq. (43), neglecting the term of $d\ln X/d\ln u_0$. Then, calculate the value of X from the value of $\bar{f}_{PP}$ by Eq. (42) as the first approximation and then obtain $d\ln X/d\ln u_0$ by log-log plot of X vs. u_0. The second approximation of $\bar{f}_{PP}$ is obtained from Eq. (43), taking account of the term $d\ln X/d\ln u_0$, and so on.

(2) Direct calculation of $D_0\rho_{s0}^2$ in RR

By the differentiation of Eq. (38) with $\bar{m} = \bar{f}_{RR} \cdot m_c$, the calculation equation is

$$\frac{d(m_c\overline{D_{rc}})}{dm_c} = D_{rc}(m_c) = 0.50\bar{f}_{RR}^{0.40}\frac{dF}{d\bar{m}} \tag{44}$$

assuming that $\bar{f}_{RR}$ is constant.

From the master curve of $\log F'u_0$ vs. $\log\bar{u}$, the value of $d\ln F/d\ln\bar{m} = d\ln F'/d\ln\bar{u}$ is calculated. From this value we obtain $\bar{f}_{RR}$ by Eq. (34) and then m_c and u_c. The direct calculation of $D\rho_s^2$ at u_c in RR is performed by Eq. (44). This calculation is possible even with the experimental data for one value of u_0.

(3) Calculation by way of the integral average diffusion coefficient.

In PP where $u_c = u_0$, the integral average diffusion coefficient is

$$\int_0^{u_c} D\rho_s^2 du = X\beta'^2 u_0/2$$

In RR

$$\int_0^{u_c} D\rho_s^2 du = 0.50 \bar{f}_{RR}^{-0.60} F' u_0$$

The values of $\int_0^{u_c} D\rho_s^2 du$ obtained from PP and RR are plotted together with u_0. Graphical differentiation of the plots gives the value of $D\rho_s^2$ as a function of u_c.

4.2 Illustration of the calculation procedure

The calculation procedure is tested with the numerical results of desorption of the PVA-water system. The master curve of the desorption rate by the superimposed plots of $F'u_0$ vs.$\bar{u}$ obtained from various u_0 values is shown in **Fig. 11**. The estimated values of $D\rho_s^2$ obtained in the above three ways respectively are shown in **Fig. 12**. The agreement between the estimated value and the value by the equation of D for the PVA-water system given in Table 1 is satisfactory.

Concluding Remarks

In the analysis of isothermal desorption (drying) of a slab, the diffusion equation expressed by the dissolved-solid coordinates is solved numerically for various type of concentration dependence of the diffusion coefficient. A method of calculating the concentration-dependent diffusion coefficient without assuming the functional form of concentration dependence is derived from an analysis of the numerical results. Based on the flux equations by the assumption of similarity of concentration distribution, the integral average diffusion coefficient is related to the desorption rate and the ratio of the average concentration to the center concentration, for both the penetration period and the regular regime. The ratios in PP and RR are empirically correlated with the desorption rates by Eqs (39) and (34) respectively. From these equations, three ways of calculating the concentration-dependent diffusion coefficient are proposed.

1) In PP, the diffusion coefficient is directly calculated by Eqs. (41), (42) and (43), using the initial slopes of E vs. $\sqrt{\tau'}$ of the desorption with various initial concentrations.

2) In RR, the diffusion coefficient is directly calculated by Eqs. (34) and (44), using the desorption rate even in single-desorption experiments.

3) Integral average diffusion coefficients are obtained by Eq. (36) for PP and Eq. (38) for RR. Graphical differentiation of these values gives the diffusion coefficient.

The error of calculation is less than 10% for the range of $0.5<(\bar{f}_{PP}$ or $\bar{f}_{RR})<0.9$, which covers the various types of concentration dependence of diffusion coefficient shown in Fig. 1 and Table 1.

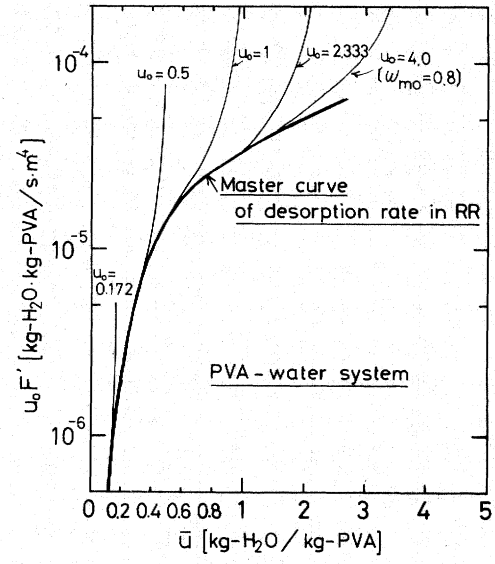

Fig. 11. Master curve of desorption rate for PVA-water system

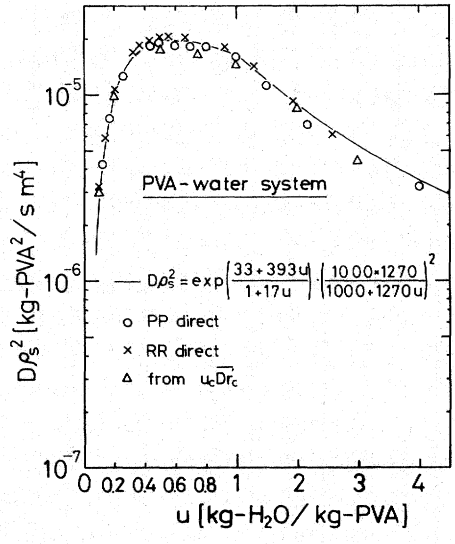

Fig. 12. Sample calculation of $D\rho_s^2$ for PVA-water system

Appendix

Derivations of Eqs. (25), (29), (36) and (41)

Eq. (25): For PP, putting Eq. (21) into Eq. (1) with Eqs. (19) and (20), we obtain

$$\frac{\partial Y}{\partial \eta} = (1-\eta)\frac{d\delta}{d\tau} f'(\eta) \tag{A-1}$$

Integrating this equation with the condition of ($\eta=0$, $Y=0$), we obtain

$$Y = -\frac{d\delta}{d\tau}\left[1 + f(\eta)(\eta-1) - \int_0^{\eta} f(\eta)d\eta\right] \tag{A-2}$$

At the surface ($\eta=1$)

$$Y(1) = F = -\frac{d\delta}{d\tau}(1-\bar{f}_{PP}) \tag{A-3}$$

Integrating Eq. (A-2), we obtain

$$\bar{Y} = \int_0^1 Y \cdot d\eta = -\frac{d\delta}{d\tau}\left[1 - 2\bar{f}_{PP} + 2\int_0^1 \eta f(\eta)d\eta\right] \tag{A-4}$$

From Eqs. (A-3) and (A-4), using Eq. (23), we obtain

$$\frac{m_c\overline{D_{r_c}}}{(1-\delta)F}=\frac{1-2\bar{f}_{PP}+2M_{PP}}{(1-\bar{f}_{PP})} \tag{A-5}$$

For the end-point of PP, Eq. (25) is obtained by setting $\delta=0$ and $m_c=1$ in Eq. (A-5).

Eq. (29): For RR where $\eta=\phi$, we also get the following equations.

$$Y=-\frac{dm_c}{d\tau}\int_0^{\phi}f(\phi)d\phi \tag{A-6}$$

$$Y(1)=F=-\bar{f}_{RR}\frac{dm_c}{d\tau} \tag{A-7}$$

$$\bar{Y}=-\frac{dm_c}{d\tau}\left[\bar{f}_{RR}-\int_0^1\phi f(\phi)d\phi\right] \tag{A-8}$$

and then we obtain Eq. (29).

Eq. (36): Eqs. (18) and (25) are assumed to hold to the point $m_c=0.99$, where

$$E=1-\bar{m}=1-0.99\cdot\bar{f}_{PP}$$

Then, from these equations, using Eq. (35), we get Eq. (36).

Eq. (41): From Eqs. (24) and (36), we obtain

$$\int_0^{u_0}D\rho_s^2du=\frac{1}{2}X\beta'^2u_0 \tag{A-9}$$

assuming $u_c=u_0$ at the end-point of PP. Differentiation of this equation by u_0 gives

$$D_0\rho_{s0}^2=\frac{1}{2}X\beta'^2\left[1+\frac{d\ln X}{d\ln u_0}+2\frac{d\ln u_0}{d\ln u_0}\right] \tag{A-10}$$

Then, using Eqs. (39) and (40), we obtain Eqs. (41), (42) and (43).

Nomenclature

a	=	parameter in mathematical model equation	[—]
D	=	(mutual) diffusion coefficient	[m^2/s]
D_0	=	reference diffusion coefficient of arbitrary value or diffusion coefficient at initial solvent concentration	[m^2/s]
D_r	=	reduced diffusion coefficient by Eq. (9)	[—]
$\bar{D}_{rc}$	=	reduced integral average diffusion coefficient by Eq. (24)	[—]
d_m	=	density of solvent	[kg/m^3]
d_s	=	density of solid	[kg/m^3]
E	=	$1-\bar{m}$, relative amount of solvent evaporated	[—]
F	=	reduced desorption rate	[—]
$\bar{f}$	=	$\int_0^1 f(\phi)d\phi=\bar{m}/\bar{m}_c$	[—]
$\bar{f}_{PP}$	=	value of f at end of penetration period	[—]
$\bar{f}_{RR}$	=	value of $\bar{f}$ during regular regime	[—]
m	=	reduced solvent content, u/u_0	[—]
R	=	half-thickness of a slab	[m]
R_s	=	half-thickness of a slab in dried state	[m]
r	=	diffusional distance	[m]
t	=	desorption time	[s]
u	=	solvent content	[kg solvent/kg solid]
X	=	value defined by Eq. (42)	[—]
Y	=	reduced flux defined by Eq. (21)	[—]
z	=	dissolved-solid coordinate defined by Eq. (6)	[kg/m^2]
Z	=	value of z at surface	[kg/m^2]
β	=	initial slope of E vs. $\sqrt{\tau}$ of penetration period	[—]
γ	=	value defined by Eq. (43)	[—]
δ	=	value of ϕ keeping initial solvent content in penetration period shown in Fig. 2	[—]
η	=	reduced distance coordinate defined by Eq. (20)	[—]
ξ	=	variable defined by Eq. (15)	[—]
ρ_s	=	solid concentration	[kg/m^3]
τ	=	reduced desorption time defined by Eq. (8)	[—]
ϕ	=	reduced dimensionless coordinate defined by Eq. (5)	[—]
ω_m	=	$u/(1+u)$, mass fraction of solvent	[—]

〈Subscript and superscript〉

c	=	refers to center value
o	=	referes to initial value
PP	=	refers to penetration period
RR	=	refers to regular regime
TP	=	refers to transition period
—	=	refers to average value

Literature Cited

1) Crank, J.: *Trans. Faraday Soc.*, **51**, 1632 (1955).
2) Crank, J.: "The Mathematics of Diffusion," 2nd ed., p. 238, Oxford Univ. Press, Oxford (1975).
3) Duda, J. L., J. S. Vrentas, S. T. Ju and H. T. Liu: *AIChE J.*, **28**, 279 (1982).
4) Van der Lijn, J.: Ph. D. Thesis, Agricultural Univ. Wageningen, The Netherlands (1976).
5) Liou, J. K. and S. Bruin: *Int. J. Heat Mass Transfer*, **25**, 1209 (1982).
6) Sano, Y., S. Yamamoto, Y. Ohtani and H. Okazaki: Proc. Kagoshima Meeting of SCEJ, A107, (1987).
7) Schoeber, W. J. A. H.: Ph. D. Thesis, Technical Univ. Eindhoven, The Netherlands, (1976).
8) Schoeber, W. J. A. H. and H. A. C. Thijssen: *AIChE Symp. Series*, **73(63)**, 12 (1977).
9) Vrentas, J. S., J. L. Duda and Y. C. Ni: *J. Polym. Sci., Polym. Physics ed.*, **15**, 2039 (1977).
10) Vrentas, J. S. and J. L. Duda: *AIChE J.*, **25**, 1 (1979).
11) Wijlhuizen, A. E., P. J. A. M. Kerkhof and S. Bruin: *Chem. Eng. Sci.*, **34**, 651 (1979).
12) Yamamoto, S., M. Hoshika and Y. Sano: Proc., 4th Int. Drying Symp., Kyoto, p. 769 (1984).